Performance Evaluation of Self-Configured Two-tier Heterogeneous Cellular Networks

Nien-Tsu Chou*, Shih-Hao Lin*, Shin-Ming Cheng*, and Shih-Hao Chang†
*Department of Computer Science and Information Engineering,
National Taiwan University of Science and Technology, Taipei 106, Taiwan.
Email: {m10115043, m10115073, smcheng}@mail.ntust.edu.tw
†Department of Computer Science and Information Engineering,
Tamkang University, New Taipei City 251, Taiwan. Email: sh.chang@ieee.org

***Abstract*—Two-tier macro/femto heterogeneous cellular networks (HCNs) have received considerable attention due to substantial improvements in high quality in-building coverage and system capacity. Distributed self-configured femtocells can be realized to mitigate inter-tier interference between macrocells and femtocells without heavy operating costs by incorporating broadcasting mechanism of macrocell. With the aid of the macrocell, who provides critical global information, femtocells can configure related parameters to achieve interference mitigation. A tractable stochastic geometry-based analytical model is proposed to evaluate of proposed self-configured scheme in terms of coverage probability. We also conduct simulation experiments according to data from OpenCellID to prove the effectiveness of the proposed self-configured scheme in the realistic two-tier HCNs.**

I. Introduction

Recent development of cellular networks directs toward high data rates and a low transmission power. To achieve that, information theory reveals the solution to be either wide communication bandwidth or a high signal to interference and noise power ratio (SINR). Consequently, the next generation communication systems, Long Term Evolution (LTE)-Advanced, deploy a larger number of base stations (BSs), such that the distance between a transmitter-receiver link can be further reduced. With lower transmission power, a high SINR can also be maintained for each link, as interference from other transmitters is reduced. This solution also avoids the conventional fixed frequency separation scheme for interference mitigation, as dividing available bandwidth into small portions significantly limits data rates. For this purpose, the heterogeneous cellular networks (HCNs) deployment [1] where low-power and small-coverage small cell BSs are distributed in the coverage of a macrocell, is considered as mandatory architecture in LTE-Advanced.

To compensate for poor indoor signal reception from the macrocell base station (abbreviated as macro-BS) in HCNs, one kind of small cell BSs, femtocell BSs (abbreviated as femto-BSs) connected by wired backhaul, are introduced to extend high quality coverage inside buildings [2]. The small coverage area of a femtocell suggests that large numbers of concurrent transmissions will increase spatial reuse, therefore potentially yielding enhanced wireless capacity. Thus, such two-tier HCNs are of tremendous interest to researchers and industry.

The main concerns in two-tier HCNs are *cross-tier interference* between macrocell and femtocells, and *intra-tier (or co-tier) interference* among femtocells, which limit the capacity improvement benefit of concurrent transmissions [3]. These problems are illustrated in Fig. 1. The random locations for user-deployed femto-BSs and the long delay of wired backhauling reduce the success of centralized interference mitigation solutions due to heavy operating costs [4]. LTE-Advanced has devoted significant standardization effort towards devising enhanced inter-cell interference coordination (eICIC) schemes for minimizing interference [5].

By acquiring additional environment information, femto-BSs can adapt their radio resources [6]–[8] or power [9], [10] to achieve interference mitigation. One possible solution is initiated by mobile station (MS), where a MS periodically performs measurement and reports to its serving femto-BS for environmental awareness and further interference mitigation [6]. However, the sensing and signaling overheads consume additional power, which is inappropriate for energy-limited mobile equipment.

In this paper, we apply an alternative approach where macro-BS broadcasts the related configurations to femto-BSs for interference mitigation. As a result, self-configuration in the two-tier HCN is achieved and femto-BSs can exploit the extra information for better performance gain. To evaluate the performance of the proposed self-configured scheme in HCNs, we propose a stochastic geometry-based analytical model [11] and focus on the performance metric of coverage probability. Different from hexagonal grid deployed BSs, stochastic geometry model for HCN [12] assumes that BSs are deployed according to Poisson Point Process (PPP) spatial model and provides lower bounds of the coverage probability of real cellular networks [13]. We further conduct a realistic experiment to evaluate the coverage probability where locations of macro-BSs follows the data provided by the open source project OpenCellID [14], [15]. To precisely simulate the clustering behaviors of femtocells in a building or apartment,

978-1-4799-0652-9/13/$31.00

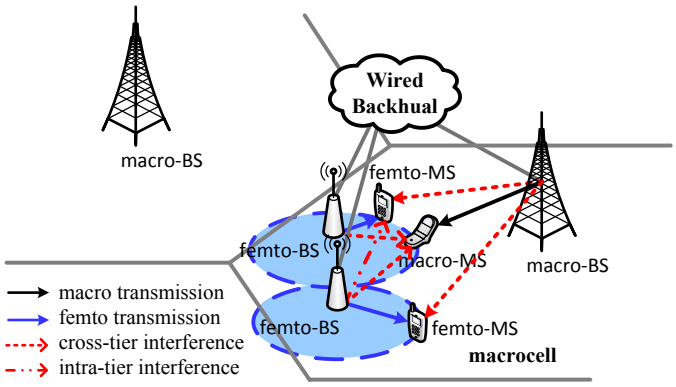

Fig. 1. Network architecture of two-tier HCN

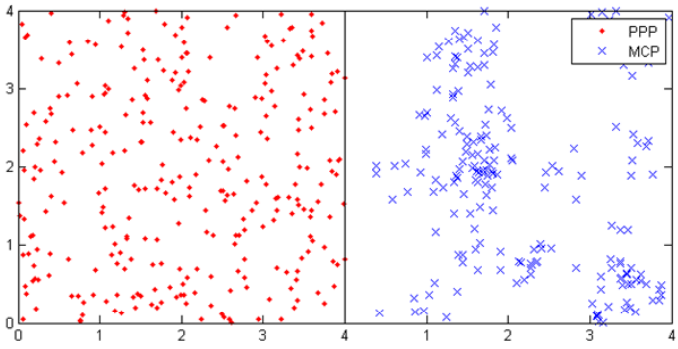

Fig. 2. BS deployments of PPP and MCP models. The system parameters are set as $\mathcal{H} = 16\text{km}^2$, $\lambda_f = 20$, $\lambda_p = 2$, $\bar{c} = 10$, $R_p = 500\text{m}$.

our simulation experiments further adopt another stochastic geometry-based models, Matern Cluster Process (MCP) [16], for accurate results of coverage probability.

The rest of the paper is organized as follows. Section II presents the system model and Section III introduces the proposed self-configured scheme and analyze the coverage probability of two-tier HCNs with self-configuration. Numerical and simulation results are provided in Section IV. Section V concludes this paper.

II. System Model

A. Network Model

As shown in Fig. 1, the downlink of an orthogonal frequency division multiple access (OFDMA) system with two-tier macro- and femtocells is considered. OFDMA-based systems typically divide system bandwidth into N basic time-frequency units of resource blocks (RBs). To achieve universal frequency reuse, both macro- and femtocells utilize the all RBs, which is known as the *co-channel* deployment. The *closed access* policy is assumed, where only subscribed femto-MS is allowed to be served by femto-BS. The unauthorized macro-MS can only be served by macro-BS even it locates within the femtocell coverage. Macro- and femto-BS respectively transmit to only one user at any given RB at full power P_m and P_f, which implies transmission power is maintained constant across the RBs. Perfect synchronization in time and frequency is assumed.

Denote $\mathcal{H} \in \mathbb{R}^2$ as the interior of a reference HCN, which consists of multiple macro-BSs of radius R_m and a macro-MS located in central of $\mathcal{H}$. The spatial distribution of macro-BSs is assumed to follow a homogeneous Poisson Point Process (PPP) with density λ_m, and the locations of the macro-BSs are denoted as $\Phi_m = \{X_i\}$. The macrocells is overlaid with femto-BSs of radius R_f, which are randomly distributed on $\mathbb{R}^2$ according to a homogeneous PPP with intensity λ_f. We let $\Phi_f = \{Y_i\}$ denote the locations of the femto-BSs.

We take into account path loss attenuation effects, Rayleigh fading with unit average power h, and background noise power per RB ρ^2 in our channel model. The path-loss exponent of transmission is denoted by α.

B. Alternative Stochastic Geometry-based Model

Typically, femtocells are deployed in a building or apartment, which implies its clustered property. In this case, Poisson Cluster Process (PCP) [17] might be an appropriate model. Poisson cluster process is defined as giving a Poisson process of parent points with density λ_p and the location of each cluster are depended on each parent point. In Matern cluster process, the number of children points in a cluster is Poisson distributed with mean $\bar{c}$ and points are uniformly centered on a parent point within a cluster region of radius R_p. As shown in Fig. 2, the considered Matern Cluster Process (MCP) model can capture the clustered behavior of femto-BSs and the density of the femto-BS λ_f applied in PPP is equivalent to $\lambda_p \bar{c}$ in MCP.

C. Metrics of Interest

In this paper, we use the *coverage probability* as the main metric of HCNs on a reference RB. The successful reception of a transmission at an MS occurs only if the SINR observed by the MS (denoted by γ) is larger than a SINR threshold (denoted by Γ). The coverage probability p_c of the typical macro-MS is defined as [13]

$$p_c = \mathbb{P}[\gamma > \Gamma]. \tag{1}$$

To guarantee the transmission quality, there is an outage constraint at the MS with maximum outage probability ϵ. Thus the outage constraint defines the minimal coverage probability, that is

$$p_c \geq 1 - \epsilon. \tag{2}$$

The second metric considered as a measure of spectral efficiency on each RB is *transmission capacity*, which is defined as the maximum density of successful transmissions satisfying a per-tier outage constraint on a reference RB [18]. Mathematically, the transmission capacity with a per-tier outage probability ϵ is

$$C = (1 - \epsilon)\lambda_\epsilon, \tag{3}$$

where λ_ϵ is the spatial density of attempted transmissions; hence, $\lambda_\epsilon(1 - \epsilon)$ is the spatial density of successful transmis-

sions.

III. Self-Configured Scheme

Since femto-BSs are paid for and maintained by customers for residential and private uses, only mobile subscribers of the femto-BS (abbrev. as femto-MSs) are allowed to establish connections with the femto-BS (known as *closed-access* policy). As a result, unauthorized MS can only connect to macro-BS (known as the macro-MS) with the received SINR

$$\gamma = \frac{P_m h \|x_i\|^{-\alpha}}{I_m + I_f + \sigma^2}, \tag{4}$$

where x_i denote the. Moreover, I_m and I_f are the intra-tier and cross-tier interference from marco-BSs and femto-BSs to the typical (reference) macro-MS located at the origin, respectively, and can be expressed as

$$I_m = \sum_{X_i \in \Phi_m} P_m h \|X_i\|^{-\alpha}; I_f = \sum_{Y_j \in \Phi_f} P_f h \|Y_j\|^{-\alpha}. \tag{5}$$

In this case, femto-BSs play the role of the pure interferers. That is, a larger number of femto-BSs necessarily leads to more severe interference (i.e., a larger I_f) and a smaller coverage probability. The proposed self-configured scheme applies *interference thinning* to control the number of active femto-BSs and thus the interference. Each femto-BS tosses a coin independently in each frame with probability $\widehat{p}$ and transmits data to corresponding femto-MS if it gets heads. Obviously, $\widehat{p}$ determines the number of active femto-BSs (i.e., $\widehat{p}\lambda_f$).

The unique overlapping feature between macro-BSs and femto-BSs in two-tier HCNs provides a solution for self-configuration of $\widehat{p}$ to achieve adaptive interference thinning. Once a femto-BS attaches or detaches the two-tier HCN (i.e., the total number of femto-BSs changes), the operator automatically calculate the adjusted $\widehat{p}$ and broadcasts it to all femto-BSs via macro-BSs. Consequently, the femto-BSs can updated $\widehat{p}$, interference is controlled, and coverage probability is preserved. Please note that such self-configuration only performed when the number of femto-BSs changes, and thus real-time updates are not needed and overheads are small.

A. Analysis of coverage probability and transmission capacity

Using the global and time-invariant information of the femto network, the operator can estimate the probability $\widehat{p}$ for interference thinning. Under the assumption that the spatial distribution of the femto-BSs follows a homogeneous PPP, the set of active femto-BSs $\Phi_f^{\widehat{p}} = \{X_n : B_n(\widehat{p}) = 1\}$ is modeled as a subset with density $\widehat{\lambda}_f = \widehat{p}\lambda_f$ where $B_n(\widehat{p})$ are i.i.d. Bernoulli random variables with parameter $\widehat{p}$. In particular, the received SINR at the reference macro-MS located at r distance away from a macro-BS guarantees

$$\mathbb{P}\left(\frac{hP_m r^{-\alpha}}{\sigma^2 + I} \geq \Gamma\right) = 1 - \epsilon. \tag{6}$$

Due to the stationary characteristic of homogeneous PPP [18], the interference measured by a typical femto-MS is representative of the interference seen by all other femto-MSs. Thus $I_m = \sum_{X_n \in \Phi_m \setminus \{X_0\}} hP_m \|X_n\|^{-\alpha}$, $I_f = \sum_{X_n \in \Phi_f^{\widehat{p}}} hP_f \|X_n\|^{-\alpha}$ is the intra-tier interference from surrounding femto-BSs to a reference femto-MS located at the origin, where h and $\|X_n\|$ are respectively the Rayleigh fading with mean 1 and the distance between the femto-BS at X_n and the typical femto-MS. According to the Lermma 1 of [12], (6) can be evaluated as

$$\begin{aligned} 1 - \epsilon = \lambda_m \int_{\mathbb{R}^2} & \exp\left(-C(\alpha)(\frac{\Gamma}{P_m})^{2/\alpha}\|x\|^2(\lambda_m P_m^{2/\alpha} + \lambda_f P_f^{2/\alpha})\right) \\ & \cdot \exp\left(-\frac{\Gamma\sigma^2}{P_m}\|x\|^\alpha\right) dx, \end{aligned} \tag{7}$$

where $C(\alpha) = \frac{2\pi^2 csc(2\pi/\alpha)}{\alpha}$. If we ignore the effect of the noise and use (7) the coverage probability is

$$\begin{aligned} \widehat{p}_c &= 1 - \epsilon \\ &= \lambda_m \int_{\mathbb{R}^2} \exp\left(-C(\alpha)(\frac{\Gamma}{P_m})^{2/\alpha}\|x\|^2(\lambda_m P_m^{2/\alpha} + \widehat{\lambda}_f P_f^{2/\alpha})\right) dx. \end{aligned} \tag{8}$$

We let $x = (x_x, x_y)$ and $T = C(\alpha)(\frac{\Gamma}{P_m})^{2/\alpha}(\lambda_m P_m^{2/\alpha} + \widehat{\lambda}_f P_f^{2/\alpha})$, then (7) becomes

$$\begin{aligned} \widehat{p}_c &= \lambda_m \int_{-\infty}^{\infty}\int_{-\infty}^{\infty} \exp\left(-T({x_x}^2 + {x_y}^2)\right) dx_x dx_y \\ &= \lambda_m \int_{-\infty}^{\infty}\int_{-\infty}^{\infty} \exp\left(-T{x_x}^2 - T{x_y}^2\right) dx_x dx_y \\ &= \lambda_m \int_{-\infty}^{\infty}\int_{-\infty}^{\infty} \exp\left(-T{x_x}^2\right)\exp\left(-T{x_y}^2\right) dx_x dx_y \\ &= \lambda_m \int_{-\infty}^{\infty} \sqrt{\frac{T}{\pi}} \exp\left(-T{x_y}^2\right) dx_y \\ &= \lambda_m \sqrt{\frac{T}{\pi}}\sqrt{\frac{T}{\pi}} \\ &= \frac{\lambda_m T}{\pi}. \end{aligned} \tag{9}$$

We put T into (9), then (9) becomes

$$\widehat{p}_c = \frac{\lambda_m\left(C(\alpha)(\frac{\Gamma}{P_m})^{2/\alpha}(\lambda_m P_m^{2/\alpha} + \widehat{\lambda}_f P_f^{2/\alpha})\right)}{\pi}. \tag{10}$$

Then we have the thining density as

$$\widehat{\lambda}_f = \frac{\frac{\widehat{p}_c \pi}{\lambda_m} - C(\alpha)(\frac{\Gamma}{P_m})^{2/\alpha}\lambda_m P_m^{2/\alpha}}{C(\alpha)(\frac{\Gamma}{P_m})^{2/\alpha} P_f^{2/\alpha}}. \tag{11}$$

The operator calculates $\widehat{p} = \widehat{\lambda}_f/\lambda_f$ as the probability for initial sensing and distributes it to all femto-BSs for self-configuration. In this case, even when all active femto-BSs transmit concurrently, the resulting intra-tier interference is still constrained. The corresponding transmission capacity C is

$$C = \widehat{p}_c\widehat{\lambda}_f = (1 - \epsilon)\widehat{\lambda}_f. \tag{12}$$

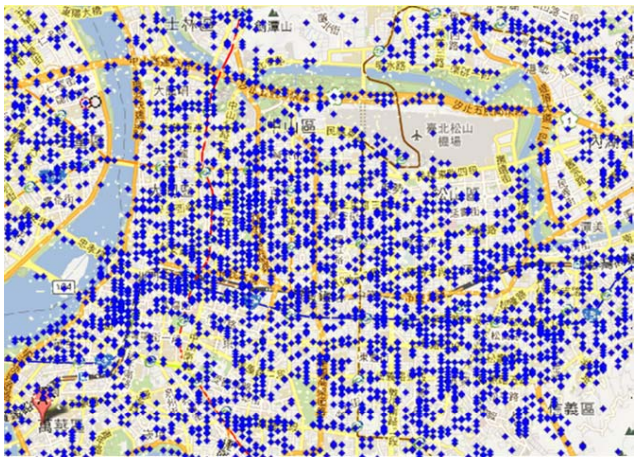

Fig. 3. Macro-BS distribution in Taipei City, Taiwan, shown on Google Map. Blue ♦s are the locations of macro-BSs.

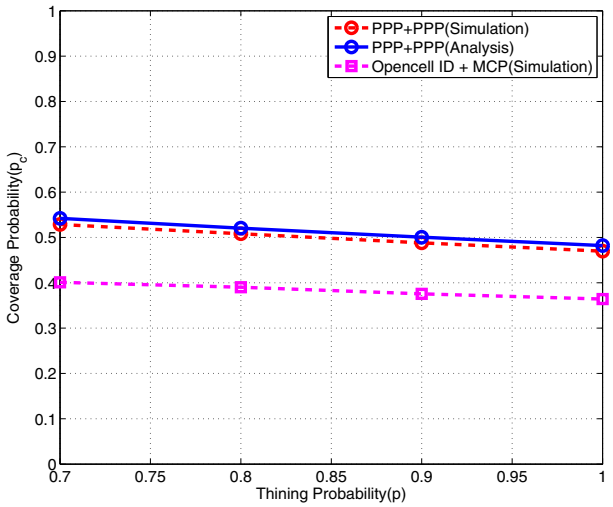

Fig. 4. Effects of the thining probability of femto-BSs on coverage probabilities

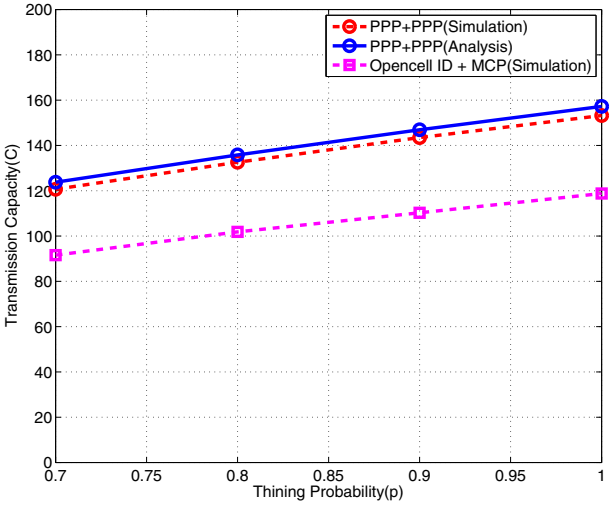

Fig. 5. Effects of the density of femto-BSs on transmission capacities with self-configuration in a reference empty RB.

IV. Performance Evaluation

This section uses investigate the performance of the proposed self-configuration scheme based on the analytical and simulation results. To comprehensively evaluate the proposed self-configuration scheme in realistic environment, this paper conducts extensively simulation experiments, where real data of macro-BSs deployments are applied with the aid of OpenCellID project [14]. Two simulation scenarios are considered as follows

- PPP+PPP: Both macro-BSs and femto-BSs are deployed by using PPP models.
- OpenCellID+MCP: The first tier macro-BSs are deployed according to the data from OpenCellID while the second tier femto-BSs are deployed following MCP model. The OpenCellID project maintains a complete and open database of macro-BS information worldwide, and we can easily retrieve latitude and the longitude information of the macro-BSs according to the target urban area. Figure 3 shows the filtered-out macro-BSs locations in Google Map of Tapiei City. Recently literature [15] shows that data of OpenCellID can facilitate the modeling of HCNs and gets reasonable results.

The simulation experiments are built on Matlab platform, and the parameter setup follows the 3GPP dual-strip model [19]. The two-tier macro/femto networks are deployed following the network model described in Section II and the details are shown in Table I. The city border we choose is [25.020284, 25.085288] of latitude, [121.490765, 121.578999] of longitude. To be able to provide better simulation environment and data reference value, we choose the urban area as 25% of Taipei city, which is the most densely populated city center.

Fig. 4 shows the effects of thinning probability $\widehat{p_c}$ on coverage probability with self-configuration. At each reference RB, every femto-BS is active/non-active according to $\widehat{p}$ calculated by the self-configured schemes. We observe that the simulation results closely match our analytical models; which implies that the analytical model is validated. This figure shows that as $\widehat{p_c}$ decreases, coverage probability significantly increases, which indicates that the thinning probability can increase coverage probability obviously.

Fig. 5 discusses the effects of thinning probability $\widehat{p}$ on C with self-configuration. It can be clearly observed that C decreases as λ_f decreases. From (11), we can obtain an appropriate density of femtocell $\widehat{\lambda}_f$ from thinning probability. Although we can select a thinning probability smaller than $\widehat{p}$ to obtain the better coverage probability (i.e., larger than $\widehat{p}_c$), transmission capacity will be smaller than $(1-\epsilon)\widehat{\lambda}_f$. As a result $\widehat{p}$ is the best one to obtain balance between coverage probability and transmission capacity.

TABLE I
PARAMETERS SETUP

	Macrocell	Femtocell
density	$\lambda_m = 65.21875$ km^{-2}	$\lambda_f = 5\lambda_m$
transmission power	$P_m = 40$W	$P_f = P_m/25 = 1.6W$
path-loss exponent	$\alpha = 3$	
noise power	$\sigma^2 = 0$	
SINR threshold	Γ = -4 db	
parent density of MCP		$\lambda_{f_p} = 10.5$ km^{-2}
number of children points of MCP		$\bar{c}_f = \lambda_f/\lambda_{f_p}$
radius of cluster region of MCP		$R_f = 0.24$ km

These figures also show that both coverage probability and transmission capacity of the realistic environment (i.e., OpenCellID+MCP) are worse than that of analytical model (i.e., PPP+PPP), which is consistent to the results in [15].

V. CONCLUSION

In two-tier macro/femto HCNs, macro-BSs can collect and broadcast time-invariant information to femto-BSs. By exploiting these features, a self-configuration scheme is proposed where macro-BSs broadcast calculated thinning probability to femto-BSs for inter-tier interference mitigation. The numerical results show that with the thinning probability, the coverage probability can be effectively controlled. To apply the proposed scheme to realistic HCNs, we conduct an extensive simulation experiment where both real position of macro-BSs are applied according to OpenCellID and clustering behaviors of femto-BSs are considered. The simulation results show that with self-configuration, interference can be mitigated in an efficient way.

ACKNOWLEDGMENTS

This work is supported in part by National Science Council, Taiwan, under contract NSC 102-2221-E-011-046-MY2.

REFERENCES

[1] A. Ghosh, N. Mangalvedhe, R. Ratasuk, B. Mondal, M. Cudak, E. Visotsky, T. A. Thomas, J. G. Andrews, P. Xia, H. S. Jo, H. S. Dhillon, and T. D. Novlan, "Heterogeneous cellular networks: From theory to practice," *IEEE Commun. Mag.*, vol. 50, no. 6, pp. 54–64, June 2012.

[2] J. G. Andrews, H. Claussen, M. Dohler, S. Rangan, and M. C. Reed, "Femtocells: Past, present, and future," *IEEE J. Sel. Areas Commun.*, vol. 30, no. 3, pp. 497–508, Mar. 2012.

[3] T. Zahir, K. Arshad, A. Nakata, and K. Moessner, "Interference management in femtocells," *IEEE Commun. Surveys Tuts.*, vol. 15, no. 1, pp. 293–311, Jan. 2013.

[4] S.-M. Cheng, S.-Y. Lien, F.-S. Chu, and K.-C. Chen, "On exploiting cognitive radio to mitigate interference in macro/femto heterogeneous networks," *IEEE Wireless Commun. Mag.*, vol. 18, no. 3, pp. 40–47, June 2011.

[5] 3GPP, "3GPP Report of TSG RAN WG1 Meeting," #62, v0.1.0, Oct. 2010.

[6] J. Xiang, Y. Zhang, T. Skeie, and L. Xie, "Downlink spectrum sharing for cognitive radio femtocell networks," *IEEE Syst. J.*, vol. 4, no. 4, pp. 524–534, Dec. 2010.

[7] Y.-S. Liang, W.-H. Chung, G.-K. Ni, I.-Y. Chen, H. Zhang, and S.-Y. Kuo, "Resource allocation with interference avoidance in OFDMA femtocell networks," *IEEE Trans. Veh. Technol.*, 2012, accepted for publication.

[8] S.-M. Cheng, W. C. Ao, F.-M. Tseng, and K.-C. Chen, "Design and analysis of downlink spectrum sharing in two-tier cognitive femto networks," *IEEE Trans. Veh. Technol.*, vol. 61, no. 5, pp. 2194–2207, May 2012.

[9] R. Madan, J. Borran, A. Sampath, N. Bhushan, A. Khandekar, and T. Ji, "Cell association and interference coordination in heterogeneous LTE-A cellular networks," *IEEE J. Sel. Areas Commun.*, vol. 28, no. 9, pp. 1479–1489, Dec. 2010.

[10] X. Chu, Y. Wu, D. Lopez-Perez, and X. Tao, "On providing downlink services in collocated spectrum-sharing macro and femto networks," *IEEE Trans. Wireless Commun.*, vol. 10, no. 12, pp. 4306–4315, Dec. 2011.

[11] M. Haenggi, J. G. Andrews, F. Baccelli, O. Dousse, and M. Franceschetti, "Stochastic geometry and random graphs for the analysis and design of wireless networks," *IEEE J. Sel. Areas Commun.*, vol. 27, no. 7, pp. 1029–1046, Sept. 2009.

[12] H. S. Dhillon, R. K. Ganti, F. Baccelli, and J. G. Andrews, "Modeling and analysis of k-tier downlink heterogeneous cellular networks," *IEEE J. Sel. Areas Commun.*, vol. 30, no. 3, pp. 550–560, Apr. 2011.

[13] J. G. Andrews, F. Baccelli, and R. K. Ganti, "A tractable approach to coverage and rate in cellular networks," *IEEE Trans. Commun.*, vol. 59, no. 11, pp. 3122–3134, Nov. 2011.

[14] "OpenCellID." [Online]. Available: http://www.opencellid.org/

[15] C.-H. Lee, C.-Y. Shih, and Y.-S. Chen, "Stochastic geometry based models for modeling cellular networks in urban areas," *Wireless Networks*, Oct. 2012.

[16] F. Baccelli, B. Blaszczyszyn, and P. Muhlethaler, "An Aloha protocol for multihop mobile wireless networks," *IEEE Trans. Inf. Theory*, vol. 52, no. 2, pp. 421–436, Feb. 2006.

[17] K. Gulati, B. L. Evans, J. G. Andrews, and K. R. Tinsley, "Statistics of co-channel interference in a field of Poisson and Poisson-Poisson clustered interferers," *IEEE Trans. Signal Process.*, vol. 58, no. 12, pp. 6207–6222, Dec. 2010.

[18] A. M. Hunter, J. G. Andrews, and S. P. Weber, "Transmission capacity of ad hoc networks with spatial diversity," *IEEE Trans. Wireless Commun.*, vol. 7, no. 12, pp. 5058–5071, Dec. 2008.

[19] 3GPP, "E-UTRA: Further Advancements for E-UTRA Physical layer aspects," 3GPP TR 36.814 v9.0.0, Mar. 2010.